20

A Non-Contact Method for Detecting On-Line Industrial Robot Position Errors

Gregory C. Smith
AI Sensors
USA

1. Introduction

To be useful, industrial robots must meet positioning accuracy requirements for their given applications. Most industrial robots can return repeatedly to the same location in space quite precisely; they typically meet published repeatability specifications on the order of 0.5 mm. On the other hand, most industrial robots cannot move as precisely to a specified (x, y, z) position in space; they typically meet published accuracy specifications roughly an order of magnitude higher (typically 10 mm or worse) (Owens, 1994).

In many cases, published repeatability specifications meet positioning accuracy needs in industrial robot applications such as spot welding, spray painting, and assembly. However, published positioning accuracy specifications often do not meet industry needs, when using off-line programming rather than manual teaching methods. As a result, to meet application positioning accuracy requirements, most robot users turn to off-line calibration to bring positioning accuracy close to robot repeatability levels (Owens, 1994). Off-line calibration generally consists of the following five steps:

1. Move the robot into several poses (positions and orientations).
2. Measure and record the precise 3D workspace coordinates of the robot tool center point (TCP) at each pose.
3. Read and record the corresponding position of the robot, from the robot controller, at each pose.
4. Use the differences between measured 3D workspace coordinates and corresponding positions read from the robot controller to correct the parameters in the kinematic model used by the controller to position the robot.
5. During robot operation, use the corrected kinematic model to compute adjusted positions in space and then command the robot to move to the adjusted positions (which causes the robot to move to the actual desired positions).

The number of calibration poses used and the corresponding link positions for each pose must be selected to provide the information needed to accurately compute the kinematic model parameters (Robinson, Orzechowski, James, & Smith, 1997). For example, Owens (1994) used 25 different poses, while Rocadas and McMaster (1997) used 50 different poses.

To measure pose positions precisely enough to complete off-line calibration, robot manufacturers generally use expensive measurement devices, such as theodolites, coordinate measurement machines, or laser tracking systems (Mayer & Parker, 1994; Nakamura, Itaya, Yamamoto, &

Source: Industrial Robotics: Programming, Simulation and Applicationl, ISBN 3-86611-286-6, pp. 702, ARS/plV, Germany, December 2006, Edited by: Low Kin Huat

Koyama, 1995; Owens, 1994). Such systems generally cannot be used for recalibrating robots in factory environments, due to cost and space limitations. However, recalibration may be needed after robot repair, collisions with the workpiece or other objects in the workspace environment, or over time as encoders or servo systems drift (Owens, 1994).

As a result, prior research offers many low-cost systems for calibrating robots off-line within factory environments. Low-cost methods for measuring robot position during calibration include cables (Owens, 1994), cameras (van Albada, Lagerberg, & Visser, 1994), dial gauges (Xu & Mills, 1999), and trigger probes with constraint planes (Zhong & Lewis, 1995).

After off-line calibration, industrial robots, run open-loop without additional control or intervention, have met the in-process accuracy needs of most current industrial applications (spot welding, material handling, workpiece handling, and assembly).

When open-loop use of robots has not met a given industrial application's needs, closed-loop control or passive compliance has been used. For example, for arc welding, laser-based vision systems have been used to locate and track welding seams (Agapakis, Katz, Friedman, & Epstein, 1990). For assembly, passive compliance devices, such as remote center compliance (RCC) devices, have been used to align components for mating (Bruyninckx et al., 2001; Boubekri & Sherif, 1990).

However, on-line sources of robot position error have been largely ignored. Collisions with the workpiece or other objects in the workplace environment, encoder errors, or servo drift can cause robot position to drift out of specification, leading to product faults, scrap, machine damage, and additional costs. Without in-process monitoring, in-process robot position errors are generally not detected until product faults are detected during product inspection.

Generally, sensors and methods used for calibrating robots cannot be used for in-process monitoring, because the mechanisms interfere with in-process robot operation (e.g., cable measuring systems, pointers, and calibration plates) or do not work well during in-process operations. Thus, typically, the only counter measures currently used to prevent in-process errors are regularly scheduled robot recalibration or production line stops when product faults are detected in inspection. However, detecting product faults after they occur is costly. Regular calibration, when not needed, is also expensive. Shop-floor recalibration of a single robot can take up to six hours or more (Owens, 1994). The wasted manpower time spent is an unnecessary excess cost.

To achieve greater operational efficiencies, new non-invasive, non-contact methods for monitoring in-process robot position are needed (Caccavale & Walker, 1997). Early work focused on using model-based methods, with existing built-in robot joint position and velocity sensors, to detect errors with respect to ideal dynamic observer or parameter estimation models (Caccavale & Walker, 1997). However, modeling accuracy, sensor characteristics, computational loads, and response times can limit the sensitivity and usefulness of model-based methods (Visinsky et al., 1994).

As an alternative, optical methods, with external sensors, such as laser systems, cameras, or machine vision systems, have also been proposed (e.g., Dungern & Schmidt, 1986). However, optical systems can also suffer from severe limitations. Laser and optical sensors can be difficult to place, since their optical paths to robot end effectors are easily blocked by workpieces or parts of the robot. In addition, smoke or sparks from welding, or fluids in other manufacturing processes, can interfere with proper laser and optical sensor operation.

2. Purpose

To overcome the limitations of optical position monitoring methods, the investigator developed a simple, low-cost method for detecting in-process robot position errors, which uses a low-cost Doppler motion detector unit placed at one or more critical robot work positions. The small detector can be easily located near critical work positions. Detector position and line of sight are not critical, since the detector measures and generates electrical signals due to large-scale robot motion, rather than precise robot end effector position.
Motion signals from the motion detector unit (MDU) are monitored as a time series, and statistical quality control methods indicate when robot position drift or other process faults occur. When faults are detected, signals can be generated to halt the robot and trigger alarms. Alarms signal the need for robot service or recalibration. Halting the robot at the earliest sign of possible position errors can help prevent product faults, scrap, machine damage, and additional costs.
The method may be more robust, in industrial environments, than optical condition monitoring methods, since radar signals can penetrate smoke, light, and other optical contaminants.

3. Experimental Setup

Figure 1 shows the experimental setup used to develop and test the proposed position error detection method. A Seiko D-TRAN RT-2000 robot was used for testing. The Seiko robot has a cylindrical configuration with four axes R (radial), T (rotational), Z (vertical), and A (gripper rotation).

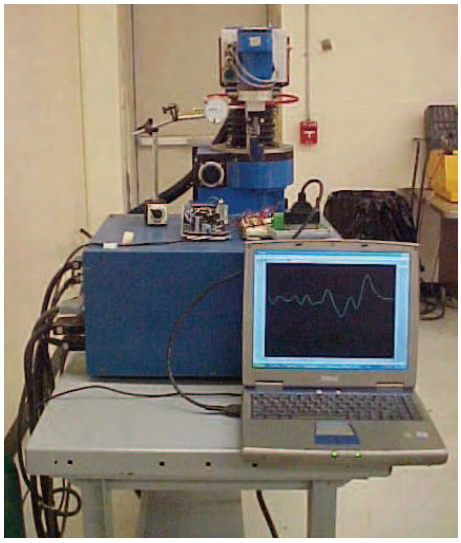

Fig. 1. Experimental setup.

Table 1 shows published repeatability and resolution specifications for each of the four robot axes. Robot reach in the R direction is 597 mm (23.5 in), maximum rotation about the T-axis is ± 145 degrees, stroke in the Z direction is 120 mm (4.72 in), and maximum rotation about the A-axis is ± 145 degrees.

The given robot controller stores a single calibration constant related to the fully extended length of the robot R axis. To calibrate the robot, the user must attach a rigid fixture, which has a precise length, to the robot and reset a stored calibration constant. Subsequently, on power-up the robot must be homed to recalibrate the robot TCP to the zero location of the workspace coordinate system. Homing moves the robot in each of the four axes to fixed limit switches and, thus, recalibrates the robot's internal servo encoders for the power-on position of the TCP zero point. Other commercial industrial robots use similar means to re-adjust the TCP to an accurate zero location. For example, Motoman, Inc. uses a special fixture (ToolSight) containing three LED sensors to re-center their welding robots (Forcinio, 1999).

Axis	Repeatability	Resolution
R	± 0.025 mm (0.001 in)	0.025 mm (0.001 in)
T	± 0.025 mm (0.001 in)	0.003 deg
Z	± 0.025 mm (0.001 in)	0.012 mm (0.0005 in)
A	± 0.025 mm (0.001 in)	0.005 deg

Table 1. Seiko D-TRAN RT-2000 repeatability and accuracy specifications.

For the experiments conducted, after robot homing, the robot was commanded to move from home position to a test point in the robot workspace coordinate system. As shown in Figure 2, a dial gauge, with a scale in English units, was used to accurately measure relative robot positions around the given test position. Figure 2 also shows the sensor circuit, composed of a Doppler radar motion detector and a low-pass filter, which was developed for measuring robot motion. The Doppler radar motion detector used was a model MDU 1620 Motion Detector Unit from Microwave Solutions (http://www.microwave-solutions.com).

Fig. 2. Sensor circuit.

The MDU 1620 is an X-band (10.525 GHz) microwave transceiver that uses the Doppler shift phenomenon to "sense" motion (Microwave Solutions, 2002). The MDU 1620 Motion Detector Unit produces an intermediate frequency (IF) output signal with frequency proportional to the velocity of the moving object. IF output signal amplitude varies as a complex function of the size and reflectivity of the sensed object and the object's distance from the MDU (Microwave Solutions, 2002).
An Omega DaqP-308 data collection system was used to sample the output signal from the Doppler motion detector/low-pass filter combination. After each command issued to move the robot from

home position to the test position, the output signal from the Doppler motion detector/low-pass filter combination was measured for 4 seconds with a 0.1 msec sampling period (10 kHz sampling frequency). As a result, according to the Nyquist Theorem, the sampled data can be used to reconstruct frequency components up to 5 kHz in the original signal (Swanson, 2000).
To prevent aliasing during sampling, an electronic filter was used to band-limit the output signal from the Doppler radar motion detector before sampling, as shown in Figure 3. The low-pass filter uses an amplifier stage to increase motion detector output signal level, a fourth-order low-pass filter stage to band limit the measured signal and to eliminate high-frequency noise, and a final amplifier stage to match the output of the filter to the input range of the data collection system.

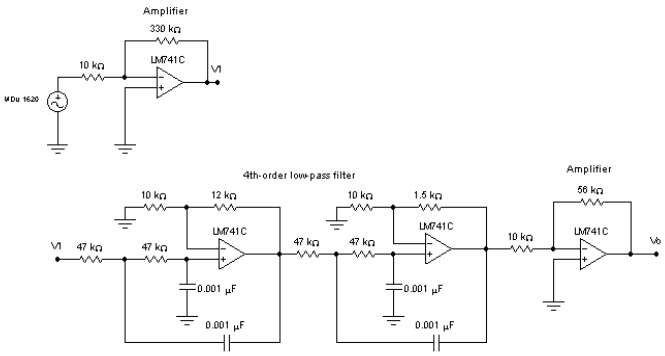

Fig. 3. Electronic filter.

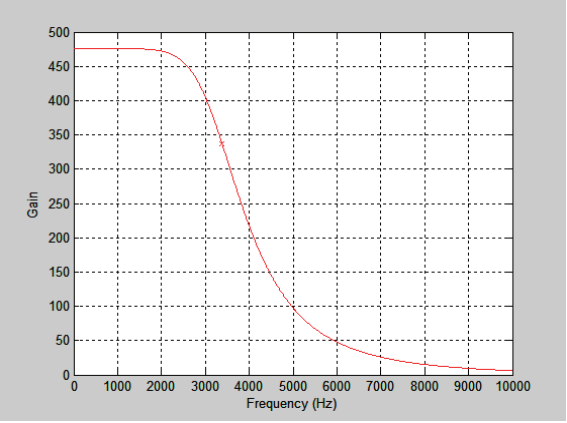

Fig. 4. Magnitude of electronic filter frequency response.

Figure 4 shows the theoretical frequency response of the filter. To meet the Nyquist sampling criterion, Swanson (2000) recommends using a band-limiting filter with an upper cut-off frequency which is roughly 0.4 times the sampling frequency. Thus, filter components were chosen such that the cut-off frequency of the fourth-order low-pass filter is 3.39 kHz (Millman & Halkias, 1972).
Captured data was analyzed using MathWorks Matlab (Version 6.5.0.1924 Release 13) and SAS JMP 5.

Five experiments were run to develop and test the proposed method for detecting on-line robot position errors in a single axis direction. Future studies will consider multi-axis robot position errors. Experiments 1 and 2 were run to verify that the robot used for testing met the manufacturer's published repeatability and resolution specifications, to verify that a dial gauge could be used to precisely measure robot position, and to characterize the drift characteristics of the robot over an extended period of cycling. Experiment 3 was run to develop a measure of robot position from sensor signals and to determine the precision of the sensor signal measure for robot moves to a single test position. Experiment 4 was run to establish a linear regression relationship between the robot position measure, which was developed in Experiment 3, and actual (induced) robot position errors. Experiment 5 was run to develop a robot position error detection model, from Experiment 3 and Experiment 4 results, and to test the prediction model for random robot moves about a single test position. The same experimental setup was used for all five experiments. The results of each experiment were used to adjust subsequent experiments, if needed. Since an incremental methodology was used, intermediate conclusions are reported with results from each experiment. Final conclusions are reported in the conclusions section at the end of the paper.

4. Experiment 1

The objectives of Experiment 1 were to:

1. Experimentally verify the repeatability of the Seiko D-TRAN RT-2000 robot used for testing,
2. Experimentally verify that a dial gauge can be used to precisely measure robot position, and
3. Experimentally determine if there is significant drift in the robot during cycling.

The method used to experimentally determine robot repeatability and drift characteristics consisted of five steps:

1. Command the robot to move to a test position 20 times,
2. Measure the position of the robot using a dial gauge,
3. Cycle the robot, between the workspace origin and the test position, for 3 hours,
4. Command the robot to move to the test position 20 times.
5. Measure the position of the robot using a dial gauge.

To simplify experimental setup and testing, the robot was moved to minimum Z-axis position, fully extended in the R-axis direction, and then commanded to move cyclically, in the T-axis direction only, between home position and a test point. The test point selected was with the robot at minimum Z-axis position, fully extended in the R-axis direction, and rotated to the 90-degree T-axis position. Minimum Z-axis position was selected to minimize distance between the sensor and the end effector, at the given test point. The fully-extended R-axis position was chosen to increase the potential for position errors, since, for the given robot, position accuracy decreases with distance from the workspace origin (Seiko, 1986). The 90-degree T-axis position was chosen so that the sensor could be mounted on the same table as the robot, to minimize potential sensor measurement errors due to robot vibrations.
Table 2 shows robot position dial gauge measurements taken at the test position before and after cycling the robot for 3 hours. Step 0, in Table 2, indicates the initial position to which the dial gauge was set, with the robot resting at the correct test position.
A one-way analysis of variance between the two groups of data shows that there is evidence of a statistically significant difference between the two group means ($\alpha = 0.05$, p-value < 0.001).

Step	Before Cycling (inches)	After Cycling (inches)
0	0.501	-
1	0.503	0.501
2	0.503	0.502
3	0.502	0.501
4	0.503	0.501
5	0.503	0.501
6	0.503	0.501
7	0.502	0.502
8	0.503	0.503
9	0.502	0.501
10	0.502	0.502
11	0.502	0.502
12	0.503	0.502
13	0.502	0.502
14	0.503	0.501
15	0.502	0.502
16	0.503	0.501
17	0.503	0.502
18	0.502	0.501
19	0.502	0.501
20	0.502	0.502

Table 2. Robot position dial gauge measurements for Experiment 1.

The mean for the Before Cycling group is 0.50243 inches (with a 95% confidence interval of 0.50216 – 0.50270 inches), and the mean for the After Cycling group is 0.501550 inches (with a 95% confidence interval of 0.50127 – 0.50183 inches). The difference between the two means is 0.00088 inches. With 95% confidence, a reasonable value for the difference between means lies between 0.00050 and 0.00126 inches. For the given robot, a reasonable value for the difference between robot position means, before and after 3 hours of cycling, lies between 0.00050 and 0.00126 inches. Experiment 1 results indicate that:

1. The robot appears to meet Seiko's published repeatability specification (0.025 mm or 0.001 inch), for measurements taken at a single time instance (before cycling or after cycling).
2. The dial gauge can be used to measure robot position precisely, (within approximately the robot repeatability specification).
3. There is evidence that the robot may drift slightly with extended cycling (3 hours). The upper limit of the 95% confidence interval for the difference between before cycling and after cycling means (0.00126 inches) is greater that the robot repeatability specification (0.001 inch), indicating that, with 95% confidence, a drift of 0.00026 inches beyond the robot repeatability specification could occur. As a result, an online method for detecting position errors might be useful for the given robot.

Since the time needed to induce a position error by cycling was relatively long, and since the magnitude of the error measured for Experiment 1 was relatively small compared to the robot repeatability specification, for Experiments 2-5, robot position errors were simulated by commanding the robot to move to positions slightly away from the test position.

5. Experiment 2

The objective of Experiment 2 was to:

1. Experimentally verify that the dial gauge could accurately detect single-axis robot position errors, for the given robot.

The method used to experimentally verify that the dial gauge could accurately detect single-axis position errors consisted of two steps:

1. Command the robot to move to the test position +/- 0.03 T-axis degrees, in 0.003 degree increments (the robot's T-axis accuracy specification is 0.003 degrees, which corresponds to 0.001 inches at the given test position).
2. Measure the position of the robot using the dial gauge.

Table 3 shows the 21 positions about the test point to which the Seiko D-TRAN RT-2000 robot was commanded to move (values in millimeters), as well as the corresponding dial gauge measurements (in inches). Note that the robot takes position commands as (x, y, z) Cartesian coordinate values, with (x, y, z) values in millimeters.

An analysis of variance shows evidence of a statistically significant relationship between dial gauge measurements and degree values ($\alpha = 0.05$, p-value < 0.0001).

Step	Position	X	Y	Dial Gauge
1	-89.970	0.313	-597.056	0.488
2	-89.973	0.281	-597.056	0.490
3	-89.976	0.250	-597.056	0.492
4	-89.979	0.219	-597.056	0.492
5	-89.982	0.188	-597.056	0.494
6	-89.985	0.156	-597.056	0.495
7	-89.988	0.125	-597.056	0.497
8	-89.991	0.094	-597.056	0.499
9	-89.994	0.063	-597.056	0.500
10	-89.997	0.031	-597.056	0.501
11	-90.000	0.000	-597.056	0.502
12	-90.003	-0.031	-597.056	0.504
13	-90.006	-0.063	-597.056	0.506
14	-90.009	-0.094	-597.056	0.507
15	-90.012	-0.123	-597.056	0.508
16	-90.015	-0.156	-597.056	0.509
17	-90.018	-0.188	-597.056	0.511
18	-90.021	-0.219	-597.056	0.513
19	-90.024	-0.250	-597.055	0.514
20	-90.027	-0.281	-597.055	0.515
21	-90.030	-0.313	-597.055	0.516

Table 3. Robot position dial gauge measurements for Experiment 2.

Equation 1 gives the equation of the least squares line shown in Figure 5:

$$\text{Predicted dial gauge value} = -41.69 - 0.4688 * \text{Robot position} \quad (1)$$

The model explains 99.74% of the variability in dial gauge measurements. Random measurement errors or other unexplained factors account for only a small amount of the observed variability in the data.

Experiment 2 results indicate that:

1. The Seiko D-TRAN RT-2000 robot appears to meet the published T-axis resolution specification (0.003 degrees). In other words, the robot can be accurately commanded to positions that differ by as little as 0.003 degrees.
2. The dial gauge can be used to detect given robot position errors to approximately the T-axis resolution specification.

Based upon Experiment 2 results, the given experimental setup was used for the remaining planned experiments.

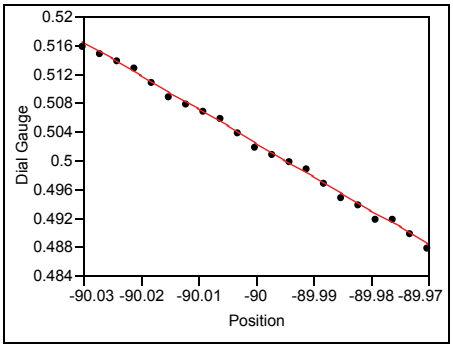

Fig. 5. Dial gauge measurements (inches) vs. robot T-axis position (degrees).

6. Experiment 3

The objectives of Experiment 3 were to:

1. Develop a measure from sensor signal samples for determining robot position,
2. Determine how well the sensor signal measure represents robot position,
3. Establish a mean signal to represent the robot moving to the correct test position, and
4. Calibrate the sensor for robot motions without position errors.

The method used to experimentally achieve Experiment 3 objectives consisted of seven steps:

1. Cycle the robot 20 times between home position and the nominal test position.
2. Measure robot position with the dial gauge.
3. Measure the sensor signal as the robot moves between home and the nominal test position. Sample the sensor signal at 0.1 msec intervals.
4. Average the values of the 20 sensor signals at each sampling time step to find the mean sensor signal value at each sampling time step.
5. Compute a root sum of squares error measure for each of the 20 sensor signals by summing squared error for each time sample with respect to the mean sensor signal value at each sampling time sample.
6. Compare standard deviation of the root sum of squares error measure for the 20 sensor signals to standard deviation of the 20 dial gauge readings.
7. Use the mean sensor signal and the standard deviation of the root sum of squares error measure as a sensor calibration standard for proper robot motion.

Figure 6 shows three representative sensor calibration signals, c_i and the mean calibration signal c_m. Figure 7 shows an expanded view of Figure 6 in the region near 2.5 seconds. The signals in Figures 6 and 7 were filtered, in Matlab, to remove any DC bias. The mean value of each signal was computed and subtracted from each of the signal's sample values.

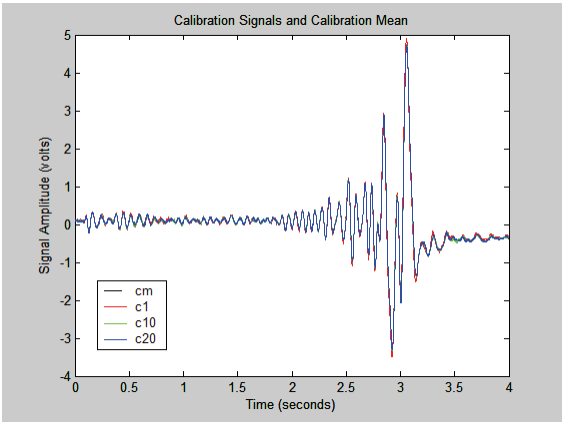

Fig. 6. Calibration signals and calibration mean.

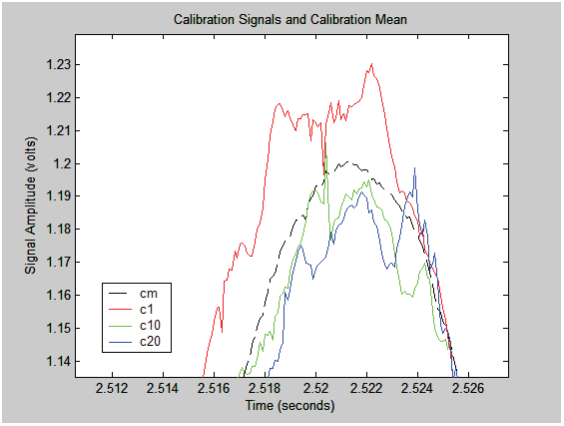

Fig. 7. Expanded view of Figure 6 near 2.5 seconds.

A frequency spectrum computed for calibration signal c_{10} shows that the sensor output signals for robot motion between home position and the test position are band limited to frequencies less than approximately 25 Hz. Therefore, the sampling period (0.1 msec) was more than adequate for accurately capturing signal content without aliasing.

To meet Experiment 3 objectives, each of the 20 filtered calibration signals were represented as an array of real numbers

$$c_i(n), \quad i = 1 \cdots 20; \; n = 1 \cdots 40000 \tag{2}$$

The mean value of all 20 signals at any given sample time step was calculated

$$c_m(n) = \frac{1}{20} \sum_{i=1}^{20} c_i(n) \tag{3}$$

As a measure of individual signal variation with respect to the mean of all 20 signals, a root-squared error value was computed for the 10,001 samples between 2.5 and 3.5 seconds

$$RSSc_i = \sqrt{\sum_{n=25000}^{35000} [c_i(n) - c_m(n)]^2} \tag{4}$$

The 10,001 samples between 2.5 and 3.5 seconds were used, rather than all 40,000 samples, to reduce computation time and to improve signal-to-noise ratio. Table 4 shows the 20 $RSSc_i$ measurements and the 20 corresponding dial gauge measurements taken for Experiment 3.

An analysis of variance indicates that there is no statistically significant relationship between $RSSc_i$ and dial gauge measurements ($\alpha = 0.05$, p-value = 0.5462). The analysis of variance indicates that, with 95% confidence, variation in both measures is probably due to random measurement error. Mean for the 20 $RSSc_i$ is 2.98, and standard deviation for the 20 $RSSc_i$ is 2.01. Mean for the 20 dial gauge measurement is 0.50015, and standard deviation for the 20 dial gauge measurements is 0.00049.

Experiment 3 results indicate that:

1. The dial gauge is a more precise method for measuring robot position at the given test point.
2. However, if the sample of 20 calibration signals accurately represents the population of all sensor signals produced by the robot moving to the given test position, the $RSSc_i$ measure developed may be usable for non-invasive non-contact in-process robot position error detection, using statistical $\overline{X}$ control chart techniques.

For the $RSSc_i$ measure to be useable as an $\overline{X}$ chart quality measure, when errors occur, individual $RSSc_i$ measures, on average, must lie at least three standard deviations from the mean for the 20 sensor calibration signals (9.01 or larger) (Besterfield, 2001).

Signal	$RSSc_i$	**Dial Gauge**
c_1	11.2241	0.500
c_2	3.2244	0.499
c_3	2.7502	0.500
c_4	3.2171	0.500
c_5	2.9028	0.500
c_6	2.3334	0.500
c_7	1.9100	0.500
c_8	1.3153	0.501
c_9	1.9060	0.500
c_{10}	2.4277	0.500
c_{11}	2.1314	0.500
c_{12}	1.9294	0.500
c_{13}	2.1702	0.501
c_{14}	2.5620	0.500
c_{15}	2.5384	0.500
c_{16}	3.0110	0.501
c_{17}	2.9737	0.501
c_{18}	3.3289	0.500
c_{19}	2.7221	0.500
c_{20}	2.9593	0.500

Table 4. Error measures for calibration signals.

7. Experiment 4

The objectives of Experiment 4 were to:

1. Determine the feasibility of using sensor signals to detect in-process robot position errors, and
2. Experimentally establish a relationship between position errors and sensor signals.

The method used to achieve Experiment 4 objectives consisted of three steps:

1. Command the robot to move from the home position +/- 0.03 T-axis degrees to the test position +/- 0.03 T-axis degrees, in 0.003 degree increments (the robot's T-axis accuracy specification is 0.003 degrees).
2. Measure the position of the robot using a dial gauge.
3. Simultaneously measure the signal (e_i) generated by the sensor.

The robot was commanded to move from offset positions about the home position to offset positions about the test position to simulate on-line position errors that would occur due to collisions with the workpiece or other objects in the workplace environment, encoder errors, or servo drift.

Data collected from Experiment 3 and Experiment 4 was analyzed using statistical methods to establish a relationship between position errors and sensor signals. The resulting relationship was then used to detect or predict on-line robot position errors (Experiment 5).

The robot was commanded to move incrementally to 21 positions about, and including, the test position. For Experiment 4, due to the time required to collect and process collected data by hand, a single replication of the experiment was conducted. However, to determine the repeatability of Experiment 4 measurements, for Experiment 5, the robot was commanded to move to the same 21 positions, but in random, rather than incremental, order.

Figure 8 shows three representative sensor error signals, e_i and the mean sensor calibration signal c_m. Figure 9 shows an expanded view of Figure 8 in the region near 2.5 seconds. Table 5 shows the 21 positions from which the robot was commanded to move, the 21 positions to which the robot was commanded to move, and the corresponding final robot workspace x-coordinate values to which the robot was commanded to move. The final robot workspace y-coordinate values were the same for all 21 positions to which the robot was commanded to move (-597.056 mm). Table 5 also shows the 21 resulting $RSSe_i$ measurements and the 21 corresponding dial gauge measurements for Experiment 4.

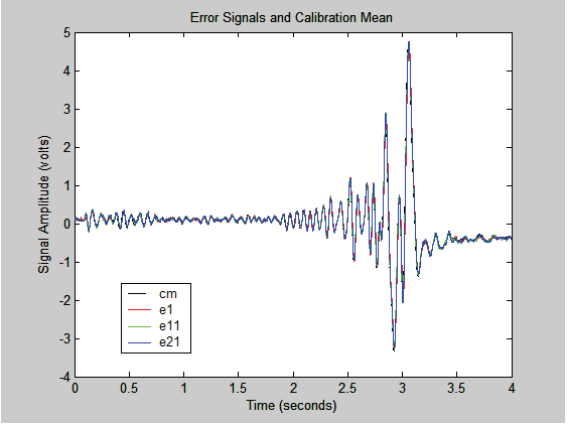

Fig. 8. Error signals and calibration mean.

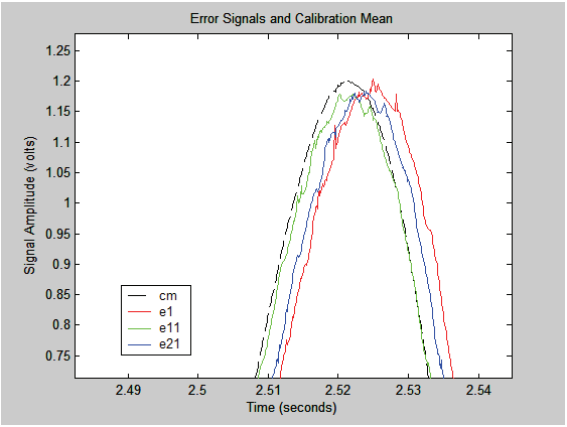

Fig. 9. Expanded view of Figure 8 near 2.5 seconds.

Signal	From	To	x-coordinate	$RSSe_i$	Dial Gauge
e_1	0.030	-89.970	0.313	24.1117	0.487
e_2	0.027	-89.973	0.281	24.0249	0.489
e_3	0.024	-89.976	0.250	23.7619	0.489
e_4	0.021	-89.979	0.219	23.5060	0.491
e_5	0.018	-89.982	0.188	22.8818	0.493
e_6	0.015	-89.985	0.156	21.1411	0.494
e_7	0.012	-89.988	0.125	20.9980	0.496
e_8	0.009	-89.991	0.094	20.6291	0.497
e_9	0.006	-89.994	0.063	21.6124	0.498
e_{10}	0.003	-89.997	0.031	21.0818	0.500
e_{11}	0.000	-90.000	0.000	5.6112	0.501
e_{12}	-0.003	-90.003	-0.031	20.9378	0.503
e_{13}	-0.006	-90.006	-0.063	19.1932	0.504
e_{14}	-0.009	-90.009	-0.094	20.5077	0.506
e_{15}	-0.012	-90.012	-0.123	17.2669	0.507
e_{16}	-0.015	-90.015	-0.156	17.1234	0.508
e_{17}	-0.018	-90.018	-0.188	16.9160	0.509
e_{18}	-0.021	-90.021	-0.219	16.6139	0.511
e_{19}	-0.024	-90.024	-0.250	16.0514	0.512
e_{20}	-0.027	-90.027	-0.281	15.0220	0.514
e_{21}	-0.030	-90.030	-0.313	13.9787	0.516

Table 5. $RSSe_i$ and dial gauge measurements for Experiment 4.

Figure 10 shows the 21 $RSSe_i$ measurements plotted as a function of the 21 corresponding final robot workspace *x*-coordinate values to which the robot was commanded to move. Figure 10 also shows the $RSSe_i$ error detection limit established in Experiment 3 (9.01). $RSSe_i$ measurements were calculated using the procedure described for Experiment 3:

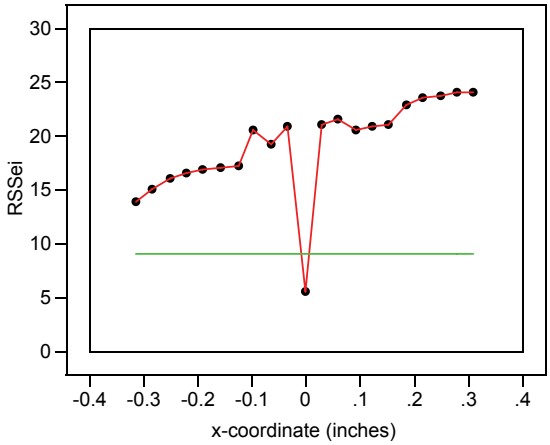

Fig. 10. $RSSe_i$ vs. robot workspace x-coordinate values.

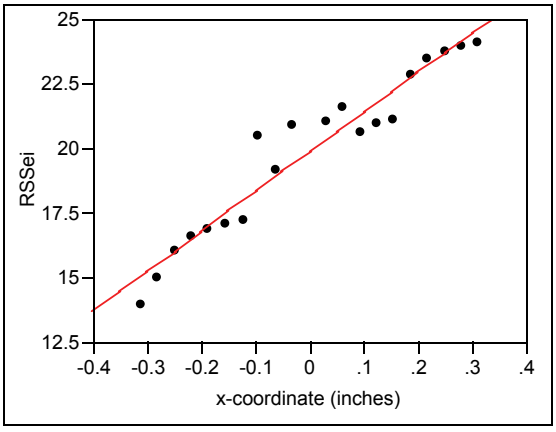

Fig. 11. $RSSe_i$ vs. robot workspace x-coordinate values for position errors.

$$RSSe_i = \sqrt{\sum_{n=25000}^{35000} [e_i(n) - c_m(n)]^2} \tag{5}$$

Figure 9 shows that sensor signals for both positive and negative final robot workspace x-coordinate values lag the calibration mean c_m, whereas e_{11}, the signal generated when the robot moves without offset from the home and test positions, closely matches the calibration mean. Both positive and negative final robot workspace x-coordinate values may lead to signals that lag the calibration mean because the generated sensor signals depend on both the distance between the sensor and the moving robot arm and the velocity of the moving robot arm.

Figure 10 shows that the $RSSe_i$ measures calculated for any of the offset robot motions exceed the single-point error limit established in Experiment 3. The method detects any induced robot position errors, to the repeatability specification of the robot. In addition, by excluding the point in Figure 10 corresponding to e_{11}, the non-error condition signal, an

analysis of variance shows evidence of a statistically significant relationship between $RSSe_i$ measurements and commanded final x-coordinate values ($\alpha = 0.05$, p-value < 0.0001). Equation 6 gives the equation of the least squares line shown in Figure 11:

$$\text{Predicted } RSSe_i = 19.87 + 15.31 * x\text{-coordinate} \quad (6)$$

The model explains 93.21% of the variability in $RSSe_i$ measurements. Random measurement errors or other unexplained factors account for only a small amount of the observed variability in the data.

Experiment 4 results indicate that:

1. Sensor signals can be used to detect single-axis on-line robot position errors at robot repeatability levels.
2. There is evidence of a statistically significant relationship between the error measure developed and actual robot position error. The relationship might allow not only detecting robot position errors, but also determining the directions and magnitudes of errors.

The original intention of the study was to develop a low-cost robust method for simply detecting on-line robot position errors. Results show that the proposed method can detect on-line position errors with 100% accuracy at robot repeatability levels. In addition, the linear relationship between the error measure developed and actual robot position error indicates that the method may provide additional capabilities, beyond position error detection.

In future studies, the proposed method can be improved by fully automating the data collection and analysis process and repeating the Experiment 3 process. In addition, the unexpected advanced error detection capabilitites of the method can be improved by replicating the Experiment 4 process to help reduce the effects unexplained variability on the linear error prediction model.

8. Experiment 5

The objective of Experiment 5 was to:

1. Test the robot position error detection model developed in Experiment 4.

The method used to test the error detection model consisted of six steps:

1. Command the robot to move from the home position +/- 0.03 T-axis degrees to the test position +/- 0.03 T-axis degrees, in 0.003 degree increments, and in random order.
2. For each move, measure the position of the robot using a dial gauge.
3. Simultaneously measure the signal (r_i) generated by the sensor.
4. Calculate the error detection measure ($RSSr_i$) for the given sensor signal.
5. For each output signal, use the developed error detection model to predict whether or not the robot was in an error condition.
6. Compare error detection model predictions to actual robot positions to determine the system's capability for detecting position errors.

Table 6 shows the 21 positions from which the robot was commanded to move, the 21 positions to which the robot was commanded to move, and the corresponding final robot

workspace *x*-coordinate values to which the robot was commanded to move. The final robot workspace *y*-coordinate values were the same for all 21 positions to which the robot was commanded to move (-597.056 mm).

Signal	From (Degrees)	To (Degrees)	X-Coordinate (Mm)	$RSSr_i$	Dial Gauge (Inches)
r_1	-0.030	-90.030	-0.313	15.5917	0.515
r_2	0.000	-90.000	0.000	6.9508	0.502
r_3	-0.027	-90.027	-0.281	15.8215	0.514
r_4	-0.015	-90.015	-0.156	19.4724	0.508
r_5	-0.024	-90.024	-0.250	16.5845	0.513
r_6	0.018	-89.982	0.188	25.6551	0.493
r_7	0.021	-89.979	0.219	25.6022	0.491
r_8	0.027	-89.973	0.281	26.9904	0.489
r_9	-0.021	-90.021	-0.219	18.4504	0.511
r_{10}	-0.018	-90.018	-0.188	18.2697	0.510
r_{11}	0.006	-89.994	0.063	22.2440	0.498
r_{12}	0.012	-89.988	0.125	23.5641	0.496
r_{13}	0.030	-89.970	0.313	27.1052	0.488
r_{14}	0.024	-89.976	0.250	25.5870	0.491
r_{15}	-0.003	-90.003	-0.031	22.8124	0.504
r_{16}	0.009	-89.991	0.094	23.5282	0.498
r_{17}	-0.009	-90.009	-0.094	20.8457	0.506
r_{18}	-0.012	-90.012	-0.123	20.3149	0.506
r_{19}	-0.006	-90.006	-0.063	22.2316	0.504
r_{20}	0.015	-89.985	0.156	24.6732	0.494
r_{21}	0.003	-89.997	0.031	23.0340	0.501

Table 6. $RSSr_i$ and dial gauge measurements for Experiment 5.

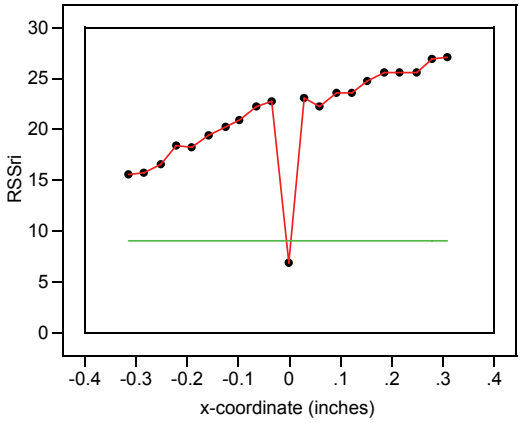

Fig. 12. *RSSri* vs. robot workspace *x*-coordinate values.

Table 6 also shows the 21 resulting $RSSr_i$ measurements and the 21 corresponding dial gauge measurements for Experiment 5.

Figure 12 shows the 21 $RSSr_i$ measurements plotted as a function of the 21 corresponding final robot workspace *x*-coordinate values to which the robot was commanded to move. Figure 12 also shows the $RSSe_i$ error detection limit established in Experiment 3 (9.01). $RSSr_i$ measurements were calculated using the procedure described for Experiment 3:

$$RSSr_i = \sqrt{\sum_{n=25000}^{35000} [r_i(n) - c_m(n)]^2} \tag{7}$$

From Experiment 3 results, the error detection model predicts a robot position error for any $RSSr_i$ value greater than 9.01. In addition, from Equation 6,

$$RSSr_i = 19.87 + 15.31 * \text{x - coordinate} \tag{8}$$

Therefore, the *x*-coordinate of the final robot position can be predicted:

$$\text{Predicted x - coordinate} = \frac{RSSr_i - 19.87}{15.31} = -1.298 + 0.0653 * RSSr_i \tag{9}$$

Finally, from the *x*-coordinate prediction, the direction and magnitude of the single-axis robot position error can also be predicted. Negative *x*-coordinate values indicate that the robot moved past the desired position; positive values indicate that the robot did not reach the desired position (with respect to the home position). The difference between the predicted and desired *x*-coordinate indicates the magnitude of the position error. For Experiment 5, the desired *x*-coordinate is always zero. Therefore, the value of the predicted *x*-coordinate indicates the magnitude of the position error.

Table 7 shows commanded (actual) and predicted *x*-coordinate values for Experiment 5. Table 7 also shows actual errors and predicted errors, whether or not the direction (sign) of the predicted error is correct, and the difference between the predicted error magnitude and the actual (induced) error magnitude (errors due to the prediction model).

Experiment 5 results show that:

1. The robot position error detection model developed in Experiment 4 predicts Experiment 5 errors with 100% accuracy, error direction with 81% accuracy, and error magnitude to within 0.223 mm.

Experiment 5 results indicate that the method developed can reliably identify robot position errors at robot repeatability levels. The method can also, to some degree, identify the direction of an error relative to the desired (commanded) position and the magnitude of the error.

In future studies, in addition to improvements recommended in Experiment 4 results, the proposed method can be improved by using standard $\overline{X}$ control chart techniques, including subgroup sampling and averaging. Using standard $\overline{X}$ control chart techniques could reduce random variation between prediction model and in-process measurements and, thereby, improve the accuracy and reliability of all three aspects of error detection and identification (error detection, error direction, and error magnitude).

Signal	Actual x-coordinate (mm)	Predicted x-coordinate (mm)	Actual Error	Predicted Error	Sign Correct	Model Error (mm)
r_1	-0.313	-0.2794	Yes	Yes	Yes	0.034
r_2	0.000	0.0000	No	No	Yes	0.000
r_3	-0.281	-0.2644	Yes	Yes	Yes	0.017
r_4	-0.156	-0.0260	Yes	Yes	Yes	0.130
r_5	-0.250	-0.2146	Yes	Yes	Yes	0.035
r_6	0.188	0.3779	Yes	Yes	Yes	0.190
r_7	0.219	0.3744	Yes	Yes	Yes	0.155
r_8	0.281	0.4651	Yes	Yes	Yes	0.184
r_9	-0.219	-0.0927	Yes	Yes	Yes	0.126
r_{10}	-0.188	-0.1045	Yes	Yes	Yes	0.084
r_{11}	0.063	0.1551	Yes	Yes	Yes	0.092
r_{12}	0.125	0.2413	Yes	Yes	Yes	0.116
r_{13}	0.313	0.4726	Yes	Yes	Yes	0.160
r_{14}	0.250	0.3734	Yes	Yes	Yes	0.123
r_{15}	-0.031	0.1922	Yes	Yes	No	0.223
r_{16}	0.094	0.2389	Yes	Yes	Yes	0.145
r_{17}	-0.094	0.0637	Yes	Yes	No	0.158
r_{18}	-0.123	0.0291	Yes	Yes	No	0.152
r_{19}	-0.063	0.1543	Yes	Yes	No	0.217
r_{20}	0.156	0.3137	Yes	Yes	Yes	0.158
r_{21}	0.031	0.2067	Yes	Yes	Yes	0.176

Table 7. Predicted vs. actual errors.

9. Conclusions

The investigator developed an non-invasive non-contact method for detecting on-line industrial robot position errors. The method uses a low-cost sensor to detect single-axis position errors. The sensor, composed of a low-cost microwave Doppler radar detector and a low-pass filter, converts robot motion into electronic signals that are A/D converted and processed using a computer.

Computer processing reduces captured signals into root-sum-of-squares error measures, with respect to a mean sensor calibration signal. Root-sum-of-squares error measures are compared to a threshold value that indicates, statistically, a 99.7% probability that an on-line position error has occurred. The threshold value can be adjusted to meet different application needs.

For the prototype constructed, and the experiments run, the sensor detected position errors with 100% accuracy, error direction with 81% accuracy, and error magnitude to within 0.223 mm.

The proposed method offers a low-cost non-invasive non-contact means for detecting on-line in-process robot position errors. Accurate in-process robot position error detection indicates the need for corrective action: robot homing, recalibration, or repair.

The proposed method offers advantages over other possible methods. The sensor developed uses a microwave Doppler radar detector, which is generally less expensive

and/or more robust in industrial environments than optical sensors, such as laser tracking systems or cameras. The proposed method is generally more practical for in-process error detection than contact devices used for robot recalibration, such as cable systems, trigger probes, or dial gauges.

The proposed method may eliminate the need for regularly scheduled robot homing or recalibration, thus improving productivity. At the same time, the proposed method identifies error conditions when they exist, reducing scrap, which also lowers costs and improves productivity.

Future proposed enhancements include:

1. Improving sensor design,
2. Improving sensor placement,
3. Detecting multi-axis position errors by choosing different sensor placement strategies or by using multiple sensors at a given position,
4. Fully automating the data collection and analysis process,
5. Using control chart techniques to improve error detection capabilities, particularly advanced error direction and error magnitude prediction capabilities, and
6. Considering different methods for removing DC bias from sensor signals.

10. References

The following references were cited to acknowledge relevant related research. They do not necessarily reflect the views or beliefs of the author.

Agapakis, J. E., Katz, J. M., Friedman, J. M., & Epstein, G. N. (1990). Vision-aided robotic welding: an approach and a flexible implementation. *International Journal of Robotics Research, 9*(5), 17-34.

Besterfield, D. H. (2001). *Quality Control, Sixth Edition*. New Jersey: Prentice-Hall.

Boubekri, N., & Sherif, W. (1999). A position control algorithm for a microcomputer controlled SCARA robot – part 1. *Computers & Industrial Engineering, 19*(1-4), 477-480.

Bruyninckx, H., Lefebvre, T., Mihaylova, L., Staffetti, E., De Schutter, J., & Xiao, J. (2001). A roadmap for autonomous robotic assembly, *Proceedings of the 4th IEEE International Symposium on Assembly and Task Planning*, Fukuoka, Japan, May 28-29, pp. 49-54.

Caccavale, F., & Walker, D. (1997). Observer-based fault detection for robot manipulators, *Proceedings of the IEEE International Conference on Robotics and Automation*, Albuquerque, NM, April, pp. 2881-2887.

Dungern, O. V., & Schmidt G. K. (1986). A new scheme for on-line fault detection and control of assembly operation via sensory information, *Proceedings of the 25th Conference on Decision and Control*, Athens, Greece, December, pp. 1891-1892.

Forcinio, H. (1999). Tighter process control ensures weld quality. *Robotics World, 17*(1), 17-20.

Mayer, J. R., & Parker, G. A. (1994). A portable instrument for 3-D dynamic robot measurements using triangulation and laser tracking. *IEEE Transactions on Robotics and Automation, 10*(4), 504-516.

Microwave Solutions (2002). *Small PCB Style - MDU1620*. Retrieved May 23, 2002, from http://www.microwave-solutions.com.

Millman, J., & Halkias, C. C. (1972). *Integrated electronics: analog and digital circuits and systems.* New York: Mc-Graw Hill.

Nakamura, H., Itaya, T., Yamamoto, K., & Koyama, T. (1995). Robot autonomous error calibration method for off-line programming system, *IEEE International Conference on Robotics and Automation*, pp. 1775-1982.

Owens, J. (1994). Robotrak: calibration on a shoestring. *Industrial Robot, 21*(6), 10-13.

Robinson, P., Orzechowski, P., James, P. W., & Smith, C. (1997). An automated robot calibration system, *IEEE International Symposium on Industrial Electronics, 1*, pp. SS285-SS290.

Rocadas, P. S., & McMaster, R. S. (1997). A robot cell calibration algorithm and its use with a 3D measuring system, *IEEE International Symposium on Industrial Electronics, 1*, pp. SS297-SS302.

Seiko Instruments USA, Inc. (1986). *Seiko D-TRAN Intelligent Robots: RT-3000 Installation, Programming, and Operation Manual*. Torrance, CA: Seiko Instruments USA, Inc.

Swanson, D. C. (2000). *Signal processing for intelligent sensor systems*. New York: Marcel Dekker.

van Albada, G. D., Lagerberg, J. M., & Visser, A. (1994). Eye in hand robot calibration. *Industrial Robot, 21*(6), 14-17.

Visinsky, M. L., Cavallaro, J. R., & Walker, I. D. (1994). Robotic fault detection and fault tolerance: a survey, *Reliability Engineering and System Safety, 46*, 139-158.

Xu, W., & Mills, J. K. (1999). A new approach to the position and orientation calibration of robots, *Proceedings of the 1999 IEEE International Symposium on Assembly and Task Planning*, Porto, Portugal, July.

Zhong, X-L., & Lewis, J. M. (1995). A new method for autonomous robot calibration, *IEEE International Conference on Robotics and Automation*.

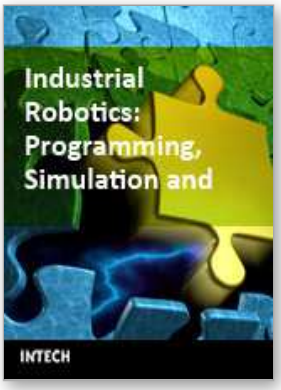

Industrial Robotics: Programming, Simulation and Applications
Edited by Low Kin Huat

ISBN 3-86611-286-6
Hard cover, 702 pages
Publisher Pro Literatur Verlag, Germany / ARS, Austria
Published online 01, December, 2006
Published in print edition December, 2006

This book covers a wide range of topics relating to advanced industrial robotics, sensors and automation technologies. Although being highly technical and complex in nature, the papers presented in this book represent some of the latest cutting edge technologies and advancements in industrial robotics technology. This book covers topics such as networking, properties of manipulators, forward and inverse robot arm kinematics, motion path-planning, machine vision and many other practical topics too numerous to list here. The authors and editor of this book wish to inspire people, especially young ones, to get involved with robotic and mechatronic engineering technology and to develop new and exciting practical applications, perhaps using the ideas and concepts presented herein.

INTECH
open science | open minds

InTech Europe
University Campus STeP Ri
Slavka Krautzeka 83/A
51000 Rijeka, Croatia
Phone: +385 (51) 770 447
Fax: +385 (51) 686 166
www.intechopen.com

InTech China
Unit 405, Office Block, Hotel Equatorial Shanghai
No.65, Yan An Road (West), Shanghai, 200040, China
中国上海市延安西路65号上海国际贵都大饭店办公楼405单元
Phone: +86-21-62489820
Fax: +86-21-62489821